

## CENTENNIAL FEATURE ARTICLE

Range Separation and Local Hybridization in Density Functional Theory<sup>†</sup>

Thomas M. Henderson, Benjamin G. Janesko, and Gustavo E. Scuseria\*

Department of Chemistry, Rice University, 6100 Main Street, Houston, Texas 77005-1892

Received: July 24, 2008; Revised Manuscript Received: September 19, 2008

Kohn–Sham density functional theory has become a standard method for modeling energetic, spectroscopic, and chemical reactivity properties of large molecules and solids. Density functional theory provides a rigorous theoretical framework for modeling the many-body exchange-correlation effects that dominate the computational cost of traditional wave function approaches. The advent of hybrid exchange-correlation functionals which incorporate a fraction of nonlocal exact exchange has solidified the prominence of density functional theory within computational chemistry. Hybrids provide accurate treatments of properties such as thermochemistry and molecular geometry. But they also exhibit some rather spectacular failures, and often contain multiple empirical parameters. This article reviews our work on developing novel exchange-correlation functionals that build upon the successes of global hybrids. We focus on more flexible functional forms, including local and range-separated hybrid functionals, constructed to obey known exact constraints and (ideally) to incorporate a minimum of empirical parametrization. The article places our work within the context of some other new approximate density functionals and discusses prospects for future work.

## 1. Introduction

During the past few decades, Kohn–Sham (KS) density functional theory<sup>1,2</sup> (DFT) has changed the way computational chemists work.<sup>3</sup> By describing complicated many-body effects within a relatively simple single-particle picture, KS-DFT provides a very attractive combination of reasonable accuracy and low computational cost. Modern functionals can be used to predict accurate ground-state structures and electronic properties in a wide variety of systems, from small organic molecules to large biological complexes to polymers and solids.

While KS-DFT has had a great many successes, it also has some spectacular failures, to the point that it is common practice to simply not use certain functionals for certain classes of problems. For example, one does not use conventional semilocal functionals (see below) to describe charge transfer excitations.<sup>4–6</sup> These failures can be attributed to the approximate exchange-correlation functionals currently in use. Ideally, we seek functionals that provide accuracy competitive with popular existing functionals while failing less often or at least less severely. A functional with broad or even universal applicability and a high degree of reliability would be a significant advance even if its accuracy were no better than what can be achieved already. To the best of our knowledge, such a functional does not yet exist, but progress is being made.

<sup>†</sup> This year marks the Centennial of the American Chemical Society's Division of Physical Chemistry. To celebrate and to highlight the field of physical chemistry from both historical and future perspectives, *The Journal of Physical Chemistry* is publishing a special series of Centennial Feature Articles. These articles are invited contributions from current and former officers and members of the Physical Chemistry Division Executive Committee and from *J. Phys. Chem.* Senior Editors.

\* To whom correspondence should be addressed. E-mail: guscus@rice.edu.

It is not clear in KS-DFT how to construct affordable functionals that give the right answers for the right reasons. We suggest that the best guide toward doing so is consideration of the underlying physics of the problem, with an eye toward satisfaction of as many relevant exact constraints as practicable. We also advocate a minimal degree of empirical parametrization; though parametrization can improve accuracy, it too often comes at the expense of obscuring the essential physics. Such guidelines have long been emphasized by our friend and collaborator, John Perdew.<sup>7</sup>

In this paper, we discuss our own efforts toward the construction of next-generation exchange-correlation functionals. We focus especially on two specific routes: range separated hybrid functionals and local hybrid functionals. Before we discuss them, however, we wish to begin with a brief overview of KS-DFT in section 2, and a discussion of self-interaction in section 3. In section 4 we present our work and touch on other recent developments in exchange-correlation functionals, before making concluding remarks in section 5.

## 2. Brief Overview of DFT

We begin with an overview of density functional theory, emphasizing a few key points that will inform our discussion of new density functional approximations. These include methods for benchmarking the performance of new functionals, the “Jacob’s ladder” of approximate density functionals,<sup>8</sup> the role of exact exchange, and the role of self-interaction error.

The foundations of density functional theory lie in the Hohenberg–Kohn (HK) theorems,<sup>9</sup> which establish that, given a ground-state electron density, it is possible in principle to extract the external potential (i.e., the potential due to the nuclei and applied electric fields) to which that density corresponds. Since the density also yields the number of electrons, we can

**Thomas M. Henderson** joined the group after a Ph.D. with Rodney Bartlett at the University of Florida and a postdoc at the Tyndall National Institute in Ireland. He has worked on range-separated and locally-range separated hybrid functionals.

**Benjamin G. Janesko** joined the group after a Ph.D. with David Yaron at Carnegie Mellon University. He has worked on local hybrid functionals and models of surface-enhanced vibrational spectroscopy.

**Gustavo E. Scuseria** is the Robert A. Welch Professor of Chemistry at Rice University. He is Associate Editor of the Journal of Chemical Theory and Computation. During the last 25 years, his research group has pioneered methodologies in coupled cluster theory, linear scaling electronic structure methods, and density functional theory, especially for periodic systems with main applications to fullerenes, carbon nanotubes, graphene nanoribbons, and bulk actinide oxides.

determine the entire Hamiltonian given only the density  $\rho(\vec{r})$ . This implies that the density in principle determines all properties of a given system, and in particular that the density determines the energy.

A second result of the HK theorems is that given an external potential  $v_{\text{ext}}(\vec{r})$ , we can obtain the ground-state energy  $E_0$  and the ground-state density  $\rho(\vec{r})$  by minimizing a functional of the density alone. That is, the exact ground-state energy is obtained by

$$E_0 = \min_{\rho} [F[\rho] + \int d\vec{r} \rho(\vec{r}) v_{\text{ext}}(\vec{r})] \quad (1)$$

and the exact ground-state density is that density which minimizes this energy expression. The functional  $F[\rho]$  contains the kinetic energy of the electrons and the electron–electron interaction energy. Unfortunately, while the HK theorems establish the existence of an energy functional, they do not tell us how to construct it. The main (but not only) difficulty lies in determining the kinetic energy, and for this purpose we turn to the Kohn–Sham scheme.

In the Kohn–Sham construction, the bulk of  $F[\rho]$  is taken from a model system of noninteracting electrons which has the same ground-state density as does the real system. The kinetic energy of the real system is then approximated by the kinetic energy of the noninteracting system, and the (hopefully small) corrections are accounted for in the exchange–correlation functional. The density is written in terms of the molecular orbitals of the noninteracting system as  $\rho(\vec{r}) = \sum_i \phi_i(\vec{r}) \phi_i(\vec{r})$ , while the total energy is obtained from

$$E_{\text{KS}}[\rho] = T_{\text{S}}[\rho] + U[\rho] + E_{\text{xc}}[\rho] + \int d\vec{r} \rho(\vec{r}) v_{\text{ext}}(\vec{r}) \quad (2)$$

Here,  $T_{\text{S}}[\rho]$  is the kinetic energy of the noninteracting system and is given by

$$T_{\text{S}}[\rho] = -\frac{1}{2} \sum_i \langle \phi_i | \nabla^2 | \phi_i \rangle \quad (3)$$

while  $U[\rho]$  is the classical Coulomb energy of the charge distribution  $\rho$

$$U[\rho] = \frac{1}{2} \int d\vec{r}_1 d\vec{r}_2 \frac{\rho(\vec{r}_1) \rho(\vec{r}_2)}{r_{12}} \quad (4)$$

with  $r_{12} = |\vec{r}_1 - \vec{r}_2|$  and  $\vec{r}_{12} = \vec{r}_1 - \vec{r}_2$ . The remaining terms not captured elsewhere are included in the exchange–correlation energy  $E_{\text{xc}}[\rho]$ . The molecular orbitals used to build the density and the kinetic energy are obtained by solving the Kohn–Sham equations

$$\left( -\frac{1}{2} \nabla^2 + v_{\text{ext}}(\vec{r}) + J(\vec{r}; \rho) + v_{\text{xc}}(\vec{r}; \rho) \right) \phi_i = \epsilon_i \phi_i \quad (5)$$

with

$$J(\vec{r}; \rho) = \frac{\delta U[\rho]}{\delta \rho(\vec{r})} \quad (6a)$$

$$v_{\text{xc}}(\vec{r}; \rho) = \frac{\delta E_{\text{xc}}[\rho]}{\delta \rho(\vec{r})} \quad (6b)$$

These simple, effective single-particle equations are similar to those of Hartree–Fock theory, and result from minimizing the energy with respect to the density (or spin-densities for functionals of the spin-densities).

Summarizing the KS procedure then, we take a trial density, construct the potentials  $J$  and  $v_{\text{xc}}$ , solve for the molecular orbitals, and last obtain the total energy from eq 2. From the molecular orbitals, we build a new density and repeat the above procedure until the density is determined self-consistently. At that point, given the exact exchange–correlation functional, the density is the exact ground-state density of the real system, and the energy obtained by eq 2 is the exact ground-state energy.

Unfortunately, the exact exchange–correlation functional in principle requires one to solve the Schrödinger equation and obtain the exact wave function. Systematic wave function-based approximations to this functional have effort comparable to the corresponding wave function treatment.<sup>10–15</sup> However, one of the main attractions of DFT is that simple approximate exchange–correlation functionals can provide accurate (albeit unsystematic) results within what is in practice a mean-field framework. Over the past several decades, an enormous body of work on such approximations has been developed. More details can be found in the extensive review of Scuseria and Staroverov.<sup>3</sup>

Before discussing approximate exchange–correlation functionals, we must introduce the criteria by which we will evaluate them. One particularly important design principle has been that approximate functionals should satisfy known constraints on the exact density functional. Another important criterion is the accuracy of a functional's predictions for properties such as molecular thermochemistry, reaction barriers, geometries, and spectroscopic properties. The performance of new approximate functionals is usually benchmarked against accurate values obtained from experiment or high-level wave function theory. For example, a functional's performance for molecular thermochemistry is often evaluated using the GN sets of Curtiss, Raghavachari, Pople, and co-workers.<sup>16–21</sup> These contain the experimental gas-phase heats of formation of several small and medium-sized molecules, along with principal ionization potentials, electron affinities, and proton affinities. We generally benchmark our functionals against the 223 heats of formation in the G3/99 set.<sup>20</sup> A functional's performance for kinetics can be tested against databases of classical reaction barrier heights, such as the HTBH38/04 hydrogen transfer<sup>22</sup> and NHTBH38/04 non-hydrogen-transfer<sup>23</sup> databases of Truhlar and co-workers. A functional's predictions for total energies can be compared against accurate ab initio energies of first- and second-row atoms.<sup>24</sup> The small, representative AE6 atomization energy and BH6 reaction barrier height test sets of Lynch and Truhlar<sup>25</sup> are invaluable for initial tests of new density functionals. Table 1 presents the results of calculations on these data sets for several representative functionals, which we describe in more detail below. Errors are defined throughout this work as theory minus experiment. Except where indicated otherwise, all results are generated using the 6-311++G(3df,3pd) basis set.

The foundation of most approximate exchange-correlation functionals is the local spin-density approximation (LSDA), which assumes that the exchange-correlation energy density  $e_{xc}$  at a point  $\vec{r}$  is equal to that of a homogeneous electron gas (HEG) whose spin-densities are equal to the spin-densities at  $\vec{r}$ . Thus, we have

$$E_{xc}^{\text{LSDA}} = \int d\vec{r} e_{xc}^{\text{HEG}}(\rho_{\uparrow}(\vec{r}), \rho_{\downarrow}(\vec{r})) \quad (7)$$

The exchange energy density for the homogeneous electron gas can be calculated exactly, and is

$$e_x^{\text{HEG}}(\rho_{\uparrow}, \rho_{\downarrow}) = -\frac{3}{4} \left( \frac{6}{\pi} \right)^{1/3} (\rho_{\uparrow}^{4/3}, \rho_{\downarrow}^{4/3}) \quad (8)$$

The correlation energy density is usually obtained from fits to Monte Carlo simulations of the homogeneous electron gas<sup>26–28</sup> with attention paid to the known high-density limit.<sup>29</sup> The LSDA is exact for constant densities and it is expected to be reasonably accurate for slowly varying densities as well.

While the LSDA is particularly simple, it is not adequate for atomic and molecular systems. As clearly indicated by Table 1, total energies are poor, and the functional is unable to describe thermochemistry or reaction barriers. The LSDA also tends to underestimate bond lengths.<sup>30,31</sup> In extended systems, band gaps are strongly underestimated.<sup>32</sup> While in finite systems the low-lying states in the electronic excitation spectrum are reasonably described,<sup>33</sup> charge transfer and Rydberg excitations are not. Thus, we must seek more sophisticated functionals.

To move beyond the LSDA, one might wish to expand the interaction in terms of fluctuations in the density. This can be done via the gradient expansion approximation, but unfortunately it is for many systems less accurate than is the LSDA<sup>34–36</sup> and in finite systems yields an exchange-correlation potential which diverges.<sup>37</sup> However, the idea of including information about the local gradient of the density is sound, and leads to generalized gradient approximations (GGAs). In a GGA, the LSDA energy density is multiplied by an enhancement factor  $F_{xc}$  which corrects for inhomogeneities of the system, so that

$$E_{xc}^{\text{GGA}} = \int d\vec{r} e_x^{\text{HEG}}(\rho_{\uparrow}, \rho_{\downarrow}) F_{xc}(\rho_{\uparrow}, \rho_{\downarrow}, \nabla \rho_{\uparrow}, \nabla \rho_{\downarrow}) \quad (9)$$

Examples of popular GGAs include the B88 exchange functional,<sup>38</sup> the LYP correlation functional,<sup>39</sup> and the PBE<sup>40</sup> and PW91<sup>41</sup> exchange-correlation functionals. [While LYP also includes the Laplacian of the density, Miehlich, Savin, Stoll, and Preuss showed that it can be recast in a form which uses only the gradient of the density by means of a partial integration (ref 42).] These generally improve on the failures of LSDA, yielding better total energies, atomization energies, and reaction barriers, and correcting (but sometimes overcorrecting) the underestimation of bond lengths.<sup>43–45</sup> Table 1 shows that the PBE exchange-correlation functional and the BLYP combination of B88 exchange and LYP correlation significantly improve upon the LSDA for thermochemistry, reaction barriers, and atomic total energies. However, their performance is still not adequate for most purposes.

Continuing up the Jacob’s ladder of functional design, we arrive at meta-GGAs, which incorporate the kinetic energy density and/or the Laplacian of the density. Examples include the functionals known as VSXC,<sup>46</sup> PKZB,<sup>47</sup> TPSS,<sup>48</sup> and M06L.<sup>49</sup> Accuracy is again improved over GGAs for energetics, and begins to be fairly reasonable. However, meta-GGAs suffer from many of the same failings as do GGAs, albeit to a lesser extent. Table 1 shows that the TPSS meta-GGA provides a moderate improvement upon the GGAs.

**TABLE 1: Mean Errors (ME) and Mean Absolute Errors (MAE) in the G3/99 Set of Heats of Formation (kcal/mol), in the HTBH38/04 and NHTBH38/04 Sets of Reaction Barrier Heights (kcal/mol), and in the Total Atomic Energies Per Electron for H–Ar ( $mE_{\text{H}}$ ) from a Variety of Functionals<sup>a</sup>**

functional	G3		HTBH38		NHTBH38		atoms	
	ME	MAE	ME	MAE	ME	MAE	ME	MAE
LSDA	-121.5	121.5	-18.1	18.1	-12.5	12.7	67.8	67.8
PBE	-21.7	22.2	-9.7	9.7	-8.5	8.6	8.6	8.6
BLYP	3.8	9.5	-7.8	7.8	-8.7	8.7	-0.6	1.2
TPSS	-5.2	5.8	-8.0	8.0	-9.0	-9.1	-2.2	2.2
B3LYP	3.5	4.9	-4.5	4.6	-4.6	4.7	-2.4	2.4
PBEh	-4.7	6.7	-4.6	4.6	-3.1	3.6	7.0	7.1
TPSSh	-0.9	5.2	-6.2	6.2	-6.9	7.6	-1.7	1.7
MPW1K	11.5	11.6	-1.0	1.5	0.4	2.0	-0.7	1.2

<sup>a</sup> We have included the LSDA, two GGAs (PBE and BLYP), a meta-GGA (TPSS), and four global hybrids (B3LYP, PBEh, TPSSh, and MPW1K).

The LSDA, GGAs, and meta-GGAs are examples of what are termed semilocal functionals, in which the exchange-correlation energy density at a point depends only on the density, its derivatives, and possibly the orbitals and their derivatives at that point. Semilocal functionals are fairly simple and efficient, but as we have seen are not sufficiently accurate. To reach acceptable accuracy, hybrid functionals, which incorporate some fraction of the exact nonlocal Hartree–Fock-type exchange, are introduced.<sup>50,51</sup> In a conventional “global” hybrid functional, the exchange-correlation energy is written as

$$E_{xc} = E_{xc}^{\text{DFA}} + c(E_x^{\text{HF}} - E_x^{\text{DFA}}) \quad (10)$$

where  $c$  is some constant parameter,  $E_x^{\text{DFA}}$  is the exchange energy from a semilocal density functional approximation (DFA), and  $E_x^{\text{HF}}$  is the nonlocal exact exchange energy, given in terms of the molecular spinorbitals of eq 5 by

$$E_x^{\text{HF}} = -\frac{1}{2} \sum_{ij}^{\text{occ}} \int d\vec{r}_1 d\vec{r}_2 \varphi_i(\vec{r}_1) \varphi_j(\vec{r}_1) \frac{1}{|\vec{r}_1 - \vec{r}_2|} \varphi_i(\vec{r}_2) \varphi_j(\vec{r}_2) \quad (11)$$

While it is possible to obtain the exact exchange potential by taking the functional derivative of the exact exchange energy with respect to the density,<sup>10,11,52,53</sup> it is not straightforward. Hybrid functionals are thus usually implemented in what is known as the generalized Kohn–Sham framework,<sup>54,55</sup> in which the nonlocal Hartree–Fock-type exchange potential is used in solving for the Kohn–Sham molecular orbitals of eq 5. Unless mentioned otherwise, this procedure is followed for all hybrids discussed in this work.

Global hybrids can be rationalized by an adiabatic connection between the real system and the noninteracting Kohn–Sham reference system<sup>50,51</sup> (section 4.4) or as a balance between self-interaction error and the simulation of nondynamical correlation effects (section 3.3). Table 1 presents results from four global hybrids: the popular B3LYP<sup>56</sup> functional (which uses 20% exact exchange), the nonempirical PBEh hybrid<sup>57,105</sup> (25% exact exchange), the TPSSh meta-GGA hybrid<sup>58</sup> (10% exact exchange), and the MPW1K hybrid,<sup>59</sup> which was optimized for kinetics and uses 42.8% exact exchange. The table illustrates that global hybrids are in general significantly more accurate than GGAs or meta-GGAs for molecular thermochemistry, with accuracy that is in many cases competitive with *ab initio* wave function methods.

The results in Table 1 illustrate some of the successes and some of the limitations of global hybrid functionals. In general,

these functionals can accurately describe either thermochemistry or reaction barriers, but not both at once (c.f. the performances of B3LYP and MWP1K in Table 1). Note, however, that some recently developed hybrids, such as those found in the M06 family of functionals,<sup>5,60</sup> achieve good compromises between accuracy for thermochemistry and for reaction barriers.

Global hybrids also fail for other important properties. Nonlinear optical properties, while improved over LSDA and GGAs, are still poor.<sup>61</sup> Dissociation of odd-electron systems, as with the LSDA and GGAs, is poorly described (see section 3.2). In extended systems, the inclusion of exact HF-type exchange is both computationally and formally problematic.<sup>62–64</sup>

All that being said, the successes of global hybrids are still remarkable, especially given their computational simplicity. In our view, new functionals should provide molecular thermochemistry that is at least competitive with B3LYP, while obeying additional exact constraints and/or providing an improved treatment of kinetics or other properties. The remainder of this article focuses on our ongoing research into functionals that repair these remaining deficiencies. Many of these deficiencies can be traced to the problem of self-interaction error (SIE) intrinsic to semilocal functionals and inherited by global hybrids. As our new functionals revolve around accounting for SIE, a brief discussion is merited.

### 3. Self-Interaction Error

Simply put, the problem of self-interaction in DFT is that most exchange-correlation functionals allow an electron to interact with itself. Traditionally, the self-interaction error has been viewed from a one-electron perspective,<sup>65</sup> through recently the importance of many-electron SIE has been emphasized.<sup>66–70</sup> We will briefly discuss them both, since considering the SIE can help guide us toward new and better functionals.

**3.1. One-Electron SIE.** A working definition of one-electron SIE is inexactness for one-electron systems. In systems with only one electron, the total electron–electron interaction must vanish. More precisely, in terms of the quantities defined of eq 2, we have

$$E_x[\rho] + U[\rho] = 0 \quad (12a)$$

$$E_c[\rho] = 0 \quad (12b)$$

That is, the electron's self-exchange cancels exactly with its self-Coulomb repulsion, and there is no correlation. Both conditions are satisfied by Hartree–Fock or other wave function approaches. However, most semilocal exchange-correlation functionals are not sufficiently flexible to ensure that these conditions are satisfied for all one-electron systems.

Unfortunately, this one-electron SIE causes problems even in many-electron systems. Because the SIE usually increases the energy and decreases as the electronic structure becomes less local, the presence of SIE tends to cause artificial stabilization of delocalized electronic states. (Though note that, as we discuss below, this delocalization can also be rationalized by considering many-electron SIE.) This delocalization leads to, for example, the well-known underestimation of reaction barriers, since the transition state is more readily delocalizable than are the reactants or products.<sup>71–74</sup> The presence of SIE causes the Kohn–Sham potential  $v_S = v_{\text{ext}} + J + v_{\text{xc}}$  to have the wrong asymptotic behavior, which leads to errors in describing charge transfer processes, Rydberg excitations, and polarizabilities and hyperpolarizabilities of long molecules.<sup>75–78</sup>

**3.2. Many-Electron SIE.** In addition to the conventional one-electron SIE, much recent attention has been paid to many-

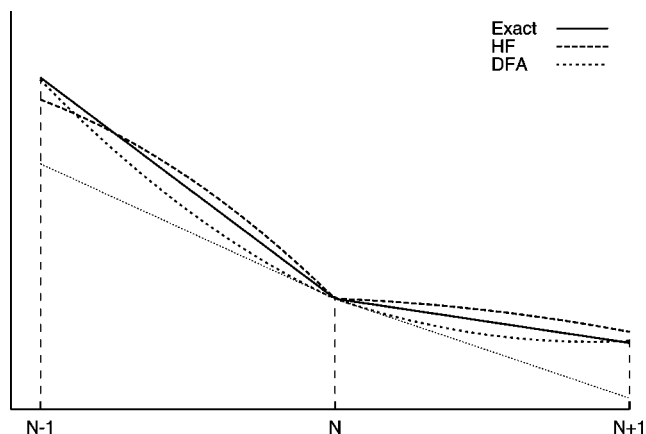


**Figure 1.** Schematic representation of the energy in a fixed external potential as a function of total electron number. The solid line represents the exact piecewise linear behavior. The dashed line represents the piecewise concave behavior of Hartree–Fock (HF), and the dotted line represents the behavior of semilocal density functional approximations (DFA). Shown in dotted lines are the straight-line approximations with the initial slope for the DFA, illustrating that there is a (small) derivative discontinuity.

electron SIE, which can be defined in terms of errors for fractionally charged subsystems. In the exact theory, the energy as a function of particle number is a piecewise linear function.<sup>79</sup> That is

$$E(N + \delta N) = (1 - \delta N)E(N) + \delta NE(N + 1) \quad (13a)$$

$$= E(N) + \delta NA(N) \quad (13b)$$

$$= E(N + 1) - (1 - \delta N)I(N + 1) \quad (13c)$$

where  $0 \leq \delta N \leq 1$  and where  $E(M)$ ,  $I(M)$ , and  $A(M)$  are respectively the ground-state energy, the principal ionization potential, and the principal electron affinity of the  $M$ -electron system. Many-electron SIE is defined as inexactness for fractional charges (that is, many-electron SIE is present when the curve  $E(N)$  is not piecewise linear and when, even if it is linear, the ionization potentials or electron affinities are incorrect).

While in the exact theory the curve of  $E(N)$  vs  $N$  is piecewise linear, for semilocal functionals, it is found to be convex.<sup>68,69</sup> That is, for a semilocal functional, we have

$$E_{\text{DFA}}(N + \delta N) < (1 - \delta N)E_{\text{DFA}}(N) + \delta NE_{\text{DFA}}(N + 1) \quad (14)$$

Semilocal functionals thus artificially favor fractionally charged fragments, by an amount defined by Yang and co-workers as the delocalization error.<sup>70</sup> For Hartree–Fock theory, the curve of  $E(N)$  vs  $N$  is instead found to be concave,<sup>68,69</sup> and

$$E_{\text{HF}}(N + \delta N) > (1 - \delta N)E_{\text{HF}}(N) + \delta NE_{\text{HF}}(N + 1) \quad (15)$$

Figure 1 schematically illustrates this behavior. Note that the piecewise linear behavior of the exact functional means that there is a discontinuity in the derivative  $dE(N)/dN$  at integer particle numbers, which generally is overestimated in Hartree–Fock theory but underestimated for semilocal functionals.<sup>68,69</sup>

The effects of many-electron SIE can be seen readily in the dissociation of homonuclear diatomic cations,  $X_2^+$ . Physically, as we increase the internuclear separation the positive charge should localize onto one nucleus or the other, and the proper dissociation limit is dissociation to  $X$  and  $X^+$ . However, since we have two degenerate states (one with the positive charge localized on the left nucleus, and one with it localized on the

right nucleus), we can take any linear combination and get the same total energy. This is just a restatement of eq 13: for all fractional charges  $\delta$  on one nucleus and  $1-\delta$  on the other, the total energy should be the same.

In a single reference method, the two relevant dissociation limits are the symmetric dissociation to  $2 X^{+1/2}$  and the symmetry-broken dissociation to  $X$  and  $X^+$ . With Hartree–Fock theory, the symmetric dissociation is higher in energy, but by relaxing the constraint on spatial symmetry, we can recover the lower energy symmetry-broken dissociation limit. The reverse is true for semilocal functionals; however, the symmetric dissociation limit is lower in energy than the symmetry-broken limit, which we cannot recover. Thus, semilocal functionals always give qualitatively incorrect depictions of these potential energy curves.

The artificial stabilization of partially charged subsystems inherent in semilocal DFT explains many common errors aside from the illustrative but not particularly relevant example of  $X_2^+$  dissociation curves. For example, NaCl dissociates improperly with semilocal functionals since for large internuclear separations such functionals favor partially charged species rather than neutral atoms (to which all A–B diatomics properly dissociate). The problem is exacerbated when we realize that, because the Coulomb interaction is treated exactly, the partially charged sodium and chlorine experience a Coulomb attraction. The dissociation curve thus not only has the wrong limit but also the wrong shape.

To the extent that subsystems with integer charge can be associated with localized electronic states, the artificial stabilization of fractionally charged subsystems suggests artificial stabilization of delocalized electronic structures, which we have already seen explains many failings of conventional functionals.

**3.3. Nondynamical Correlation and SIE.** Given the errors introduced by SIE, it may appear unreasonable to use semilocal approximations for the exchange–correlation functional. Semilocal exchange functionals seem particularly unreasonable, given that exact exchange is computationally inexpensive (in molecules), free of one-electron SIE, and properly dissociates homonuclear diatomic cations  $X_2^+$ . It turns out that semilocal exchange functionals can mimic important nondynamical correlation effects that would otherwise require computationally expensive correlated calculations. From this point of view, the success of hybrid functionals is a consequence of their ability to balance the undesirable effects of SIE with the desirable simulation of nondynamical correlation that is intrinsic to semilocal exchange functionals.

We illustrate this with the exchange and correlation holes<sup>80</sup> of a simple covalent bond, the  $H_2$  molecule. The exchange–correlation hole formalism is discussed in Appendix A. Briefly, in an  $N$ -electron system, a reference electron at point  $\vec{r}$  interacts with the other  $N - 1$  electrons. This interaction can be partitioned into the reference electron's classical Coulomb interaction with all  $N$  electrons (eq 4), and its interaction with an exchange–correlation “hole” about  $\vec{r}$  containing  $-1$  electrons. The exchange–correlation hole thus corrects for one-electron SIE (i.e., the difference between a reference electron's interaction with all  $N$  electrons, contained in  $U[\rho]$ , and its interaction only with the other  $N - 1$  electrons.).

Figure 2 presents the exact exchange, exact exchange–correlation, and LSDA exchange holes about the point  $\vec{r}$  in symmetric singlet  $H_2$ . [Results are evaluated in the limit of infinite internuclear separation.] The exact exchange hole is delocalized across both atoms. However, the exact exchange–correlation hole is localized to the atom containing the reference

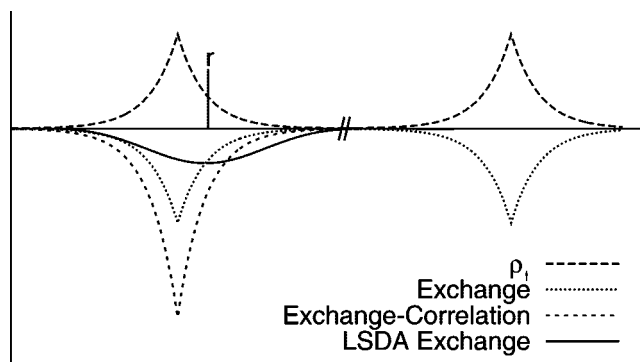


**Figure 2.** Exchange–correlation holes in stretched singlet  $H_2$ , evaluated for a  $\uparrow$ -spin reference electron at point  $\vec{r}$ . The electron density  $\rho_1$  is included for comparison. Spatial symmetry of the wave function is enforced (i.e., we use the restricted Hartree–Fock determinant to define the exchange hole). Note that the wave function is evaluated in the limit of infinite H–H separation, with a finite H–H separation shown for convenience.

electron.<sup>81</sup> This corresponds to nondynamical “left–right” correlation: when the reference electron is at a point  $\vec{r}$  on the left atom, the other electron localizes to the right atom, and vice-versa. The LSDA exchange hole is localized about  $\vec{r}$  by construction, and thus mimics the effects of left–right correlation. On the other hand, in the  $H_2^+$  homonuclear diatomic cation, the exact exchange hole becomes the exact exchange–correlation hole, such that the LSDA hole is qualitatively incorrect.

We note that one can recover a localized exchange hole within Hartree–Fock theory by allowing a symmetry-broken wave function with, e.g., the  $\uparrow$  electron localized to the left atom and the  $\downarrow$  electron localized to the right atom. Breaking symmetry, in other words, allows the exact exchange hole to mimic exact exchange plus nondynamical correlation. However, while breaking symmetry yields a localized exact exchange hole in this case, it is not a panacea and cannot properly describe all nondynamical correlation effects. This gives a different perspective on the many-electron SIE discussed above.

#### 4. Next-Generation Functionals

It is fair to say that the advent of hybrid functionals is responsible for the current popularity of DFT in the chemistry community. While B3LYP is still the most popular functional in computational chemistry, there has been a great deal of progress in the last 15 years in developing more flexible hybrid functional approximations. We will discuss some of these new approximations here, focusing on our own work. Below we present detailed discussions of our range-separated, local, and local-range-separated hybrid functionals. We also touch on some other developments (nondynamical correlation functionals, adiabatic connection functionals, and exploring the limits of empiricism) that provide particularly interesting complements to our work. [Much of the work done on hybrid functionals by other groups is omitted here due to space limitations.] Note that we will henceforth be suppressing explicit spin dependence for brevity of notation.

Our recent work in functional development has focused on two generalizations of hybrid functionals: range-separated hybrids<sup>63,75,76,78,82–88</sup> as pioneered by Savin and co-workers<sup>82–84</sup> and local hybrids,<sup>89–93</sup> with recent attention paid to their combination. The exchange–correlation hole of a global hybrid functional (c.f. eq 10) can be written as

$$h_{xc}(\vec{r}_1; \vec{r}_{12}) = h_{xc}^{\text{DFA}}(\vec{r}_1; \vec{r}_{12}) + c(h_x^{\text{HF}}(\vec{r}_1; \vec{r}_{12}) - h_x^{\text{DFA}}(\vec{r}_1; \vec{r}_{12})) \quad (16)$$

where  $h_x^{\text{HF}}$ ,  $h_x^{\text{DFA}}$ , and  $h_{xc}^{\text{DFA}}$  are respectively the exact exchange hole, a semilocal exchange hole, and a semilocal exchange-correlation hole. This follows from the linearity of the exchange-correlation energy in the exchange-correlation hole, as expressed in eq A-7. While exchange-correlation holes for many semilocal functionals have not been provided, prescriptions for their construction at the GGA<sup>94–96</sup> and meta-GGA<sup>97</sup> level are available.

The basic idea of range-separated and local hybrids is that there is no formal requirement that  $c$  be a constant. Rather, range-separated hybrids write

$$h_{xc}^{\text{RSH}}(\vec{r}_1; \vec{r}_{12}) = h_{xc}^{\text{DFA}}(\vec{r}_1; \vec{r}_{12}) + c(r_{12})(h_x^{\text{HF}}(\vec{r}_1; \vec{r}_{12}) - h_x^{\text{DFA}}(\vec{r}_1; \vec{r}_{12})) \quad (17)$$

while local hybrids employ

$$h_{xc}^{\text{LH}}(\vec{r}_1; \vec{r}_{12}) = h_{xc}^{\text{DFA}}(\vec{r}_1; \vec{r}_{12}) + c(\vec{r}_1)(h_x^{\text{HF}}(\vec{r}_1; \vec{r}_{12}) - h_x^{\text{DFA}}(\vec{r}_1; \vec{r}_{12})) \quad (18)$$

Extensions to  $c(\vec{r}_1, r_{12})$  are also possible. These more flexible forms can more precisely tune the balance between self-interaction error and inclusion of nondynamical correlation effects. We discuss particular range-separated and local hybrid functionals below.

**4.1. Range-Separated Hybrids.** We have introduced range-separated hybrids in terms of exchange-correlation hole models above. An alternative way of thinking about the same form is in terms of separating the electron–electron interaction into different components and then treating the components separately. Historically, this is how range-separated hybrids have usually been presented. Most often, the electron–electron repulsion operator is separated into short-range (SR) and long-range (LR) pieces, as

$$\frac{1}{r_{12}} = \underbrace{\frac{\text{erfc}(\omega r_{12})}{r_{12}}}_{\text{SR}} + \underbrace{\frac{\text{erf}(\omega r_{12})}{r_{12}}}_{\text{LR}} \quad (19)$$

Here, erf is the standard error function, erfc is its complement, and  $\omega$  is a parameter which controls the range of the separation. As  $\omega$  approaches zero (infinity) the long-range (short-range) interaction vanishes. While there is no requirement that the error function be used to define short-range and long-range interactions, it is a convenient choice as the integrals required can be evaluated analytically in both Gaussian and plane-wave basis sets.

Once these two interactions are defined, different methods are used for each range. Since both wave function theory and density functional theory treat  $U[\rho]$  in the same way, this term is unaffected. The exchange and correlation interactions, however, differ. Our discussion will focus on exchange, but note that range-separated correlation functionals are also in use,<sup>82,84,99–104</sup> primarily as a route toward combining the precise wave function description of the long-range and the efficient and accurate DFT treatment of the short-range.

Given a short-range and a long-range interaction, the range-separated hybrid form for  $E_{xc}$  becomes

$$E_{xc}^{\text{RSH}} = E_{xc}^{\text{DFA}} + c_{\text{SR}}(E_x^{\text{SR-HF}} - E_x^{\text{SR-DFA}}) + c_{\text{LR}}(E_x^{\text{LR-HF}} - E_x^{\text{LR-DFA}}) \quad (20)$$

Here,  $E_x^{\text{SR-HF}}$  and  $E_x^{\text{LR-HF}}$  are the short-range and long-range Hartree–Fock-type exchange energies, while  $E_x^{\text{SR-DFA}}$  and  $E_x^{\text{LR-DFA}}$  are the short- and long-range semilocal exchange energies. The exact exchange components are obtained from two-electron integrals in the usual way, while the semilocal pieces are obtained from exchange hole models. For the short-range pieces, we thus have

$$E_x^{\text{SR-HF}} = -\frac{1}{2} \sum_{ij}^{\text{occ}} \int d\vec{r}_1 d\vec{r}_2 \varphi_i(\vec{r}_1) \varphi_j(\vec{r}_1) \times \frac{\text{erfc}(\omega r_{12})}{r_{12}} \varphi_i(\vec{r}_2) \varphi_j(\vec{r}_2) \quad (21a)$$

$$E_x^{\text{SR-DFA}} = \frac{1}{2} \int d\vec{r}_1 d\vec{r}_2 \rho(\vec{r}_1) h_x^{\text{DFA}}(\vec{r}_1; \vec{r}_{12}) \frac{\text{erfc}(\omega r_{12})}{r_{12}} \quad (21b)$$

with analogous expressions for the long-range terms.

Many semilocal functionals do not provide a model for the exchange hole  $h_x^{\text{DFA}}(\vec{r}_1; \vec{r}_{12})$ , in which case one needs to be developed. Commonly used models for the exchange hole include the GGA exchange hole model of Ernzerhof and Perdew,<sup>94</sup> the meta-GGA exchange hole model of Constantin, Perdew, and Tao,<sup>97</sup> and the general-purpose LSDA-based model of Iikura and co-workers.<sup>75</sup> We have recently introduced a GGA exchange hole model intended specifically for use in range-separated hybrids,<sup>95</sup> and many other exchange hole models have also been proposed, including a recent model suggested by Bahmann and Ernzerhof.<sup>96</sup>

Typically, range-separated hybrids fall into one of two categories: screened hybrids and long-range-corrected hybrids. Screened hybrids use exact exchange only for small  $r_{12}$ , while long-range-corrected hybrids use exact exchange for large  $r_{12}$ . Our research group has introduced functionals of both types, based on the Ernzerhof–Perdew model for the PBE exchange hole,<sup>94</sup> along with a recently proposed compromise functional which uses exact exchange for intermediate  $r_{12}$  instead.

**4.1.1. HSE Screened Hybrid.** The nonempirical PBEh<sup>57,105</sup> global hybrid, though somewhat inferior to B3LYP in molecules, is generally superior for solids, possibly because unlike B3LYP, it is exact for uniform densities. Unfortunately, the computational demands of PBEh can become prohibitive for extended systems or for macromolecules because the exact exchange interaction decays rather slowly as a function of  $r_{12}$ , particularly as the band gap (HOMO–LUMO gap in molecules) becomes small. This long-range nature of exact exchange causes significant computational burden over conventional semilocal functionals in large systems. Moreover, in metallic systems, the long-range exact exchange is actually unphysical, or, more precisely, is approximately canceled by the long-range RPA correlations.<sup>29,62,106,107</sup> For both of these reasons, Heyd, Scuseria, and Ernzerhof introduced the HSE screened hybrid.<sup>63,86,108–110</sup>

The HSE functional writes the exchange-correlation energy as

$$E_{xc}^{\text{HSE}} = E_{xc}^{\text{PBE}} + \frac{1}{4}(E_x^{\text{SR-HF}} - E_x^{\text{SR-PBE}}) \quad (22)$$

where  $E_x^{\text{SR-PBE}}$  is the short-range PBE exchange energy. In terms of our exchange-hole expression of eq 17, we therefore have

$$c(r_{12}) = \frac{1}{4} \operatorname{erfc}(\omega r_{12}) \quad (23)$$

At  $\omega = 0$ , the HSE functional becomes identical to PBEh, whereas at  $\omega = \infty$ , it becomes identical to PBE. Larger values of  $\omega$  provide greater computational efficiency, but if  $\omega$  is too large, the error becomes unacceptable. The latest (HSE06)<sup>86</sup> version of the functional uses  $\omega = 0.11a_0^{-1}$  as an acceptable compromise, with  $a_0$  the Bohr radius.

Table 2 shows some benchmark results for thermochemistry, reaction barriers, and total energies, for comparison with the corresponding numbers in Table 1. For molecular systems, HSE gives results of the same caliber as the PBEh hybrid. This is as we would expect, since the range  $r_0$  over which HSE uses a significant fraction of exact exchange is  $r_0 \sim 1/\omega \sim 9a_0$ , which is on the order of three or four chemical bonds. The differences between HSE and PBEh (see Table 1) are due to the fact that the exchange hole model upon which HSE is constructed does not exactly reduce to PBE. For the G3 set, HSE and the global hybrid of the PBE hole functional give essentially identical predictions (data not shown).

More interesting is the performance of HSE for solids. Semilocal functionals are well-known to consistently underestimate band gaps,<sup>32</sup> whereas the inclusion of exact exchange raises the band gap.<sup>111,112</sup> The screened exact exchange in HSE is apparently the right amount to give band energy differences in excellent agreement with optical band gaps in semiconductors. An extensive study of forty systems<sup>110</sup> shows that while the LSDA and PBE band energy differences underestimate the optical band gap by more than 1 eV, HSE is in error by only 0.25 eV, though it still tends to underestimate the gap.

In addition to band gaps, HSE also improves upon semilocal functionals for the prediction of lattice constants,<sup>110</sup> formation of point defects in silicon,<sup>113</sup> and for the description of rare earth oxides.<sup>114–117</sup> Paier and co-workers have recently shown that in solids, HSE gives lattice constants, bulk moduli, and cohesive energies similar to those from the PBEh hybrid and dramatically superior to those predicted by B3LYP.<sup>64,118</sup>

While HSE gives predictions comparable to global hybrids in molecules, and is as good as or better than global hybrids in solids, the screened exchange interaction has another significant advantage. By reducing the range over which the exact exchange must be computed, HSE becomes significantly more computationally efficient in solids and large molecules than are conventional global hybrids, both for energetics and for properties.<sup>109</sup>

**4.1.2. LC- $\omega$ PBE Long-Range-Corrected Hybrid.** While the HSE functional is computationally much more efficient in large systems than are conventional hybrids, it suffers from the weaknesses of semilocal functionals for quantities sensitive to the long-range exchange potential and the self-interaction error in density tails. In order to correct this, an entirely opposite approach can be taken, and this was the choice made by Vydrov

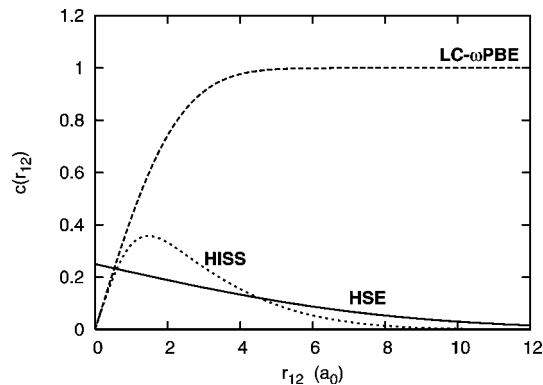


**Figure 3.** Fraction of exact exchange as a function of interelectronic separation  $r_{12}$  for three range-separated hybrid functionals.

and Scuseria in their LC- $\omega$ PBE functional.<sup>78</sup> Here, the exchange-correlation energy is written as

$$E_{xc}^{\text{LC-}\omega\text{PBE}} = E_x^{\text{SR-PBE}} + E_x^{\text{LR-HF}} + E_c^{\text{PBE}} \quad (24)$$

where  $E_x^{\text{LR-HF}}$  is the long-range exact exchange energy. We thus have

$$c(r_{12}) = \operatorname{erf}(\omega r_{12}) \quad (25)$$

in terms of the exchange hole expression of eq 17. The single empirical parameter is set to  $\omega = 0.4a_0^{-1}$ , which is thermochemically optimum. Note that as  $\omega$  approaches 0, the functional approaches PBE, while as  $\omega$  approaches infinity, the functional becomes exact exchange with PBE correlation.

As Table 2 reveals, LC- $\omega$ PBE gives excellent performance both for thermochemistry and for reaction barriers, in contrast to simple global hybrids. Other functionals can make this claim as well, but they generally rely on extensive empirical parametrization to do so, while LC- $\omega$ PBE uses only one parameter. Apparently, exact exchange at large interelectronic separations is quite important, but not so relevant at shorter distances. We note that in the absence of significant long-range correlation effects, the exact exchange hole is equal to the exact exchange-correlation hole at large interelectronic separations. We also note that the exchange potential given by LC- $\omega$ PBE is the exact long-range exchange-correlation potential in atoms and molecules. These two observations may help explain the success of LC- $\omega$ PBE for finite systems.

Aside from accuracy for thermochemistry and reaction barriers, LC- $\omega$ PBE has many other desirable properties related to its correct long-range exchange potential. Because LC- $\omega$ PBE gives an exchange potential with the correct asymptotic behavior, it is much more accurate for such quantities as molecular polarizabilities and other nonlinear optical properties than are semilocal functionals or global hybrids.<sup>78</sup>

Interestingly, LC- $\omega$ PBE seems to have low many-electron SIE. Although it does not properly dissociate homonuclear diatomic cations  $X_2^+$ , predicting the symmetric dissociation into  $2 X^{+1/2}$  to be favored over dissociation to  $X + X^+$ ,<sup>68</sup> it predicts the two limits to be much closer together than do semilocal functionals or global hybrids.<sup>78</sup> Unlike such functionals, LC- $\omega$ PBE predicts that NaCl dissociates to neutral atoms, and it correctly predicts the distance at which the intramolecular charge transfer occurs.<sup>78</sup>

Given its simplicity, reliability, and accuracy for atomic and molecular systems, we strongly recommend LC- $\omega$ PBE for those applications. In extended systems, however, its inclusion of 100% long-range exact exchange is problematic. In such cases,

**TABLE 2: Mean Errors and Mean Absolute Errors in the G3/99 Set of Heats of Formation (kcal/mol), in the HTBH38/04 and NHTBH38/04 Sets of Reaction Barrier Heights (kcal/mol), and in the Total Atomic Energies Per Electron for H–Ar ( $mE_H$ ) from a Variety of Range-Separated GGAs**

functional	G3		HTBH38		NHTBH38		atoms	
	ME	MAE	ME	MAE	ME	MAE	ME	MAE
HISS	2.5	4.3	-1.3	1.7	-0.2	1.8	4.5	4.8
HSE	-2.1	4.9	-4.6	4.6	-3.5	3.9	6.1	6.2
LC- $\omega$ PBE	-0.9	4.2	-0.5	1.3	1.4	2.4	4.4	5.0

another approach is necessary, and one possibility is to use a multirange hybrid, as described next.

**4.1.3. HISS Three-Range Functional.** The HSE and LC- $\omega$ PBE functionals have very different physical content, and are in some sense complementary: HSE is best suited to large systems, whereas LC- $\omega$ PBE is better suited to molecules. Ideally, we would like to combine the advantages of the two functionals, and this is the motivation behind the three-range functional of Henderson, Izmaylov, Scuseria, and Savin (HISS).<sup>119,120</sup> Since both HSE and LC- $\omega$ PBE give good molecular thermochemistry, the HISS functional writes the exchange-correlation energy as

$$E_{xc}^{\text{HISS}} = E_{xc}^{\text{PBE}} + c_{\text{MR}}(E_x^{\text{MR-HF}} - E_x^{\text{MR-PBE}}) \quad (26)$$

with  $E_x^{\text{MR-HF}}$  and  $E_x^{\text{MR-PBE}}$  respectively the middle-range exact exchange and middle-range PBE exchange energies. These are defined in terms of a three-range partitioning of the Coulomb operator, as

$$\frac{1}{r_{12}} = \underbrace{\frac{\text{erfc}(\omega_{\text{SR}} r_{12})}{r_{12}}}_{\text{SR}} + \underbrace{\frac{\text{erf}(\omega_{\text{LR}} r_{12})}{r_{12}}}_{\text{LR}} + \underbrace{\frac{1 - \text{erfc}(\omega_{\text{SR}} r_{12}) - \text{erf}(\omega_{\text{LR}} r_{12})}{r_{12}}}_{\text{MR}} \quad (27)$$

so that the fraction of exact exchange becomes

$$c(r_{12}) = c_{\text{MR}}(1 - \text{erfc}(\omega_{\text{SR}} r_{12}) - \text{erf}(\omega_{\text{LR}} r_{12})) \quad (28)$$

The parameters  $\omega_{\text{SR}}$ ,  $\omega_{\text{LR}}$ , and  $c_{\text{MR}}$  are determined by fits to small test sets of atomization energies and barrier heights, subject to the constraints that band gaps in a small set of solids are reproduced with acceptable accuracy. This results in  $\omega_{\text{SR}} = 0.84a_0^{-1}$ ,  $\omega_{\text{LR}} = 0.20a_0^{-1}$ , and  $c_{\text{MR}} = 0.6$ . In Figure 3 we show the functions  $c(r_{12})$  defining the amount of exact exchange included as a function of range for HISS, HSE, and LC- $\omega$ PBE.

The HISS functional apparently combines many of the advantages of HSE and of LC- $\omega$ PBE. As can be seen from Table 2, HISS performs as well as does LC- $\omega$ PBE for thermochemistry, reaction barriers, and atomic total energies. In particular, like LC- $\omega$ PBE, HISS is substantially more accurate for reaction barrier heights than is HSE. On the other hand, while HSE predicts semiconductor band gaps in excellent agreement with experiment, LC- $\omega$ PBE overestimates them by about 4 eV, as is to be expected due to its inclusion of long-range exact exchange.<sup>120</sup> Though not as accurate for band gaps as is HSE, HISS overestimates them and is comparable to, but slightly better than, PBEh. That HISS delivers accurate reaction barriers while also giving qualitatively correct electronic structures for extended systems suggests that it may be an ideal functional for use in studying quantities such as reactions at metal surfaces, in which both extended systems and finite subsystems play a role.

**4.2. Local Hybrids.** Position-dependent admixture of exact exchange provides another approach to tuning the amount of exact exchange in a hybrid functional, and the corresponding balance between SIE and nondynamical correlation. The total exchange-correlation energy in this local hybrid formalism is obtained from eq 18 as

$$E_{xc}^{\text{LH}} = E_{xc}^{\text{DFA}} + \int d\vec{r} c(\vec{r})(e_x^{\text{HF}}(\vec{r}) - e_x^{\text{DFA}}(\vec{r})) \quad (29)$$

Here,  $e_x^{\text{HF}}(\vec{r})$  and  $e_x^{\text{DFA}}(\vec{r})$  are the exact exchange energy density and a semilocal exchange energy density, respectively. The

mixing function  $c(\vec{r})$  tunes the fraction of exact exchange incorporated at the point  $\vec{r}$ . The exact exchange energy density is defined by

$$E_x^{\text{HF}} = \int d\vec{r} e_x^{\text{HF}}(\vec{r}) \quad (30)$$

and can be evaluated explicitly (in the conventional gauge, see below) following eq 11 as

$$e_x^{\text{HF}}(\vec{r}) = -\frac{1}{2} \sum_{ij}^{\text{occ}} \varphi_i(\vec{r}) \varphi_j(\vec{r}) \int d\vec{r}' \frac{\varphi_i(\vec{r}') \varphi_j(\vec{r}')}{|\vec{r} - \vec{r}'|} \quad (31a)$$

$$= -\frac{1}{2} \int d\vec{r}' \frac{|\rho_1(\vec{r}; \vec{r}')|^2}{|\vec{r} - \vec{r}'|} \quad (31b)$$

Here

$$\rho_1(\vec{r}; \vec{r}') = \sum_i^{\text{occ}} \varphi_i(\vec{r}) \varphi_i(\vec{r}') \quad (32)$$

is the one-particle density matrix of the Kohn–Sham reference system. (The density matrix introduced in eq 32 is central to much of our recent work on local hybrids, as discussed below.) The semilocal exchange energy density is evaluated as in eq 9. Equation 30 implies a “gauge freedom” in the exchange energy density, as any energy density

$$\tilde{e}_x^{\text{HF}}(\vec{r}) = e_x^{\text{HF}}(\vec{r}) + \Delta(\vec{r}) \quad (33)$$

is valid as long as  $\Delta(\vec{r})$  integrates to zero.<sup>121</sup> The effect of this gauge freedom on the performance of local hybrids has not been extensively investigated.

The general local hybrid form of eq 29 was suggested by Burke and co-workers<sup>89</sup> as early as 1998, but specific forms of the mixing function  $c(\vec{r})$  were not proposed or implemented until later.<sup>8,90</sup> Jaramillo, Scuseria, and Ernzerhof<sup>90</sup> proposed and implemented a local hybrid with

$$c(\vec{r}) = \frac{\tau_{\text{w}}(\vec{r})}{\tau(\vec{r})} \quad (34)$$

$$\tau_{\text{w}}(\vec{r}) = \frac{|\nabla \rho(\vec{r})|^2}{8\rho(\vec{r})} \quad (35)$$

This mixing function incorporates no exact exchange in regions of constant density (e.g. the homogeneous electron gas) where semilocal exchange is exact, and 100% exact exchange in one-electron regions where exact exchange provides the exact exchange-correlation functional. Unfortunately its thermochemical performance is rather poor.<sup>90</sup> Later, Kaupp and co-workers<sup>92,122,123</sup> showed that empirically parametrized mixing functions including

$$c(\vec{r}) = \alpha \frac{\tau_{\text{w}}(\vec{r})}{\tau(\vec{r})} \quad (36)$$

and

$$c(\vec{r}) = \text{erf}(\beta s) \quad (37)$$

where  $s$  is the reduced density gradient ( $s = |\nabla \rho|/2k_{\text{F}}\rho$ , with the Fermi wave vector  $k_{\text{F}} = (3\pi^2\rho)^{1/3}$ ), provide accurate thermochemistry and reaction barriers in local hybrids of LSDA exchange (see Table 3). The empirical parameters  $\alpha = 0.48$  and  $\beta = 0.22$  are optimized for thermochemistry. Unfortunately, comparable accuracy has not been reached in local hybrids of GGA and meta-GGA exchange. Local hybrids have been implemented self-consistently within the LHF/CEDA<sup>124,125</sup> approximation to the optimized effective potential,<sup>10–12,53,54,126</sup> by Kaupp and co-workers.<sup>127,128</sup> These authors have also recently



**TABLE 3: Mean and Mean Absolute Errors in the G3/99 Set of Heats of Formation (kcal/mol), the HTBH38/04 and NHTBH38/04 Sets of Reaction Barrier Heights (kcal/mol), and the Total Energies Per Electron of the Atoms H–Ar (mE<sub>H</sub>), for Some Local Hybrid Functionals**

functional	G3		HTBH38		NHTBH38		atoms	
	ME	MAE	ME	MAE	ME	MAE	ME	MAE
Lh-LSDA, $\tau_w/\tau$ (ref 90)	129.0	129.1	16.2	16.2	10.8	11.0	-8.8	12.8
Lh-LSDA, 0.48 $\tau_w/\tau$ (ref 122)	0.0	3.8	-1.6	2.1	-1.5	2.4	30.8	30.8
Lh-LSDA, $1-\Pi^{\text{LSDA}}$ (ref 91)	-1.4	14.8	0.5	2.8	2.0	4.2	29.0	29.0
Lh-PBE, $(1-\Pi^{\text{PBE}})^2$ (ref 93)	5.6	7.1	-4.5	4.5	-3.8	4.1	6.8	7.0
Lh-LSDA, $(1-\Pi)^{\zeta}(\tau_w/\tau)^{\gamma}$ (ref 93)	-1.4	4.9	-3.4	3.7	-2.7	3.9	51.4	51.4

investigated the adiabatic connection as a route to more physically motivated local hybrids.<sup>129</sup>

Much of our recent work on local hybrids exploits the one-particle density matrix introduced in eq 32. In an effort to build more physically motivated local hybrid mixing functions, we compare the Kohn–Sham density matrix used to construct the exact exchange energy density of eq 31b, with the model density matrices that are implicit in semilocal exchange functionals. The simplest such semilocal model density matrix occurs in the LSDA. It is the exact one-particle density matrix of a homogeneous electron gas with electron density  $\rho(\vec{r})$

$$\begin{aligned} \rho_1^{\text{HEG}}(\rho, u) &= \frac{1}{(2\pi)^3} \int d\vec{k} e^{-i\vec{k}\cdot\vec{u}} \\ &= \frac{1}{2\pi^2} \left( \frac{\sin(k_F u)}{u^3} - \frac{k_F \cos(k_F u)}{u^2} \right) \end{aligned} \quad (38)$$

Substituting  $\rho_1^{\text{HEG}}(\rho, u)$  into eq 31 returns the LSDA exchange energy density of eq 7. (Recall that spin-dependence has been suppressed throughout this work.)

We have proposed a “density matrix similarity metric” that compares the density matrices used to construct exact and semilocal exchange at points  $\vec{r}$ .<sup>91</sup> For LSDA, the metric is defined as

$$\Pi^{\text{LSDA}}(\vec{r}) = \frac{1}{\rho(\vec{r})} \int d\vec{r}_{12} \rho_1(\vec{r}; \vec{r} + \vec{r}_{12}) \rho_1^{\text{HEG}}(\rho(\vec{r}), r_{12}) \quad (39)$$

The metric has a number of useful properties. It is bound between zero and one by the Cauchy–Schwarz inequality. It is one in the homogeneous electron gas where  $\rho_1 = \rho_1^{\text{HEG}}$ , and zero in molecular density tails where LSDA is a poor approximation. Reference 91 shows that it can be evaluated analytically from the Kohn–Sham orbitals in a Gaussian basis set. It can be extended to any semilocal exchange functional that is constructed from a model density matrix, allowing us to “customize” the local hybrid mixing function of particular semilocal functionals. In ref 93, we used the LSDA-based exchange hole model of Hirao and co-workers<sup>75</sup> to construct a model density matrix and similarity metric for PBE exchange.

We have used this metric to construct local hybrid mixing functions  $c(\vec{r})$  (eq 29). Our initial work focuses on local hybrids that use a large fraction of exact exchange in regions where the semilocal model density matrix has a low similarity to the exact Kohn–Sham density matrix. Figure 4 illustrates the parameter-free  $1-\Pi^{\text{LSDA}}(\vec{r})$  mixing function and the one-parameter mixing function of eq 35 evaluated along the bond axis of N<sub>2</sub>. Table 3 presents representative results for five local hybrid functionals: an LSDA local hybrid with the mixing function of eq 34, the accurate one-parameter LSDA local hybrid of eq 36, a local hybrid of LSDA exchange using the density matrix similarity based mixing function  $1-\Pi^{\text{LSDA}}(\vec{r})$ , a local hybrid of PBE exchange using a one-parameter mixing function  $(1-\Pi^{\text{PBE}}(\vec{r}))^2$ ,

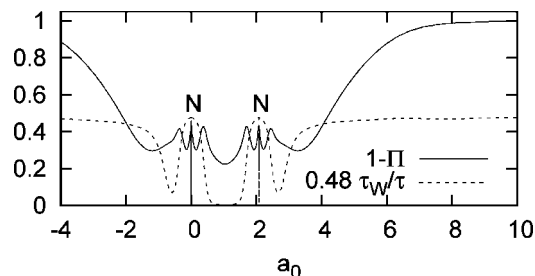


**Figure 4.** Local hybrid mixing functions  $1-\Pi^{\text{LSDA}}(\vec{r})$  and  $0.48\tau_w/\tau$  evaluated along the N–N bond axis of N<sub>2</sub>. Nuclear positions are labeled.

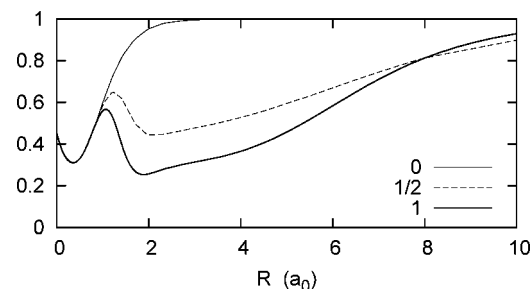


**Figure 5.**  $1-\Pi^{\text{LSDA}}(\vec{r})$  in Li atom containing 0, 1/2, or 1 valence electrons. Results are plotted vs the distance  $R$  from the nucleus.

and a more complicated two-parameter mixing function that combines our similarity metric with eq 34. [Results in Table 3 are calculated post-LSDA, with details as in refs 91 and 93.] The parameter-free  $1-\Pi^{\text{LSDA}}$  mixing function significantly improves on the parameter-free  $\tau_w/\tau$  mixing function, though it is still inadequate for thermochemistry. However, its successors give rather reasonable results, suggesting that this line of investigation is worth pursuing.

Table 3 also demonstrates that the LSDA local hybrids give poor total atomic energies. While the results are better than LSDA (Table 1), they are worse than any other functional tested here. Interestingly, the total atomic energies are significantly improved for both the PBE local hybrid and the  $\tau_w/\tau$  LSDA local hybrid incorporating 100% HF exchange in atomic cores. We suggest that these total energy errors may result from deficiencies in the LSDA description of atomic cores.

One of the most notable properties of our density matrix similarity metrics is their sensitivity to fractional occupancy. The exact exchange hole of a system containing  $0 < \delta < 1$  electrons is normalized to  $-\delta$ , while semilocal model exchange holes are always normalized to  $-1$ . Given this, we expect that the similarity of eq 39 should be relatively small for fractionally occupied regions. Figure 5 illustrates this for a Li atom with 0, 1/2, or 1 valence electrons. [The fractionally occupied system in Figure 5 is obtained from symmetric Li<sub>2</sub> with a very long Li–Li bond.] The similarity metric of eq 38 is unaffected in the core region, but changes dramatically in the valence region. As expected, the similarity is relatively small ( $1-\Pi^{\text{LSDA}}(\vec{r})$  is

**TABLE 4: Mean and Mean Absolute Errors in the G3/99 Set of Heats of Formation (kcal/mol), the HTBH38/04 and NHTBH38/04 Sets of Reaction Barrier Heights (kcal/mol), and the Total Energies Per Electron of the Atoms H–Ar ( $mE_H$ ) for Screened (SC) and Long-Range-Corrected (LC) Local Hybrids of LSDA Exchange**

functional	G3		HTBH38		NHTBH38		atoms	
	ME	MAE	ME	MAE	ME	MAE	ME	MAE
SC-Lh-LSDA	2.9	5.0	-1.3	2.1	-0.9	2.2	26.3	26.4
LC-Lh-LSDA	-0.5	3.9	-1.6	2.2	-0.5	2.3	29.4	29.9

relatively large) when the valence region is fractionally occupied. This property may makes these similarity metrics useful for more sophisticated treatments of many-electron self-interaction error.

**4.3. Local Range Separation.** We have seen that both local and range-separated hybridization can extend on global hybrids. While neither approach significantly improves upon the thermochemical performance of global hybrids, both approaches can simultaneously provide accurate thermochemistry and accurate reaction barriers. Additionally, local and range-separated hybrids can be designed to satisfy more known exact constraints than do conventional global hybrids. An interesting new direction is to combine the two approaches to build local range separated hybrids. There are at least two ways to proceed: local admixture of range-separated exact exchange with a fixed range-separation parameter, and range-separated hybrids in which the range-separation parameter  $\omega$  is chosen to be spatially dependent. We will briefly consider both approaches. In either case, we must define the short-range and long-range exact-exchange and semilocal exchange energy densities. In the exact exchange case, we have formally

$$e_x^{\text{SR-HF}}(\vec{r}, \omega) = -\frac{1}{2} \sum_{ij} \varphi_i(\vec{r}) \varphi_j(\vec{r}) \int d\vec{r}' \varphi_i(\vec{r}') \varphi_j(\vec{r}') \times \frac{\text{erfc}(\omega|\vec{r} - \vec{r}'|)}{|\vec{r} - \vec{r}'|} \quad (40)$$

while for semilocal functionals we have instead

$$e_x^{\text{SR-DFA}}(\vec{r}, \omega) = \frac{1}{2} \int d\vec{u} \rho(\vec{r}) h_x^{\text{DFA}}(\vec{r}; \vec{u}) \frac{\text{erfc}(\omega u)}{u} \quad (41)$$

with corresponding results for long-range. Again, attention must be paid to issues of gauge.

**4.3.1. Local Admixture of Range-Separated Exact Exchange.** This implementation of local range separation combines a global range-separation parameter  $\omega$  with a position-dependent admixture of exact exchange. We have thus far explored two limiting cases: long-range-corrected local hybrids incorporating 100% long-range exact exchange and screened local hybrids incorporating no long-range exact exchange.<sup>131</sup> Respectively, these give us

$$E_{\text{xc}}^{\text{LC-LH}} = E_x^{\text{SR-DFA}} + E_x^{\text{LR-HF}} + E_c^{\text{DFA}} + \int d\vec{r} c(\vec{r}) (e_x^{\text{SR-HF}}(\vec{r}) - e_x^{\text{SR-DFA}}(\vec{r})) \quad (42)$$

and

$$E_{\text{xc}}^{\text{SC-LH}} = E_{\text{xc}}^{\text{DFA}} + \int d\vec{r} c(\vec{r}) (e_x^{\text{SR-HF}}(\vec{r}) - e_x^{\text{SR-DFA}}(\vec{r})) \quad (43)$$

These functionals are a straightforward generalization of the local hybrids of eq 29, requiring only that the exchange energy densities be evaluated with the screened interaction. Table 4

presents preliminary thermochemical results. The table shows screened and long-range-corrected local hybrids of LSDA exchange, using the one-parameter mixing function of Eqn. 36. The screened local hybrid uses  $\alpha = 0.55$ ,  $\omega = 0.11a_0^{-1}$ , and the long-range-corrected hybrid uses  $\alpha = 0.44$ ,  $\omega = 0.18a_0^{-1}$ . The results in Table 4 indicate that both screened and long-range-corrected local hybrids of LSDA exchange can give thermochemistry and kinetics comparable to the corresponding local hybrid of full-range LSDA exchange (row 2 of Table 3), though both also suffer from the poor description of total energies. [Results in Table 4 are calculated self-consistently, with details as in ref 131.]

**4.3.2. Range Separated Hybrids with Local  $\omega$ .** This approach is somewhat more complicated operationally, though not formally. Here, we write the exchange-correlation energy as

$$E_{\text{xc}} = E_{\text{xc}}^{\text{DFA}} + c_{\text{SR}} \int d\vec{r} [e_x^{\text{SR-HF}}(\vec{r}, \omega(\vec{r})) - e_x^{\text{SR-DFA}}(\vec{r}, \omega(\vec{r}))] + c_{\text{LR}} \int d\vec{r} [e_x^{\text{LR-HF}}(\vec{r}, \omega(\vec{r})) - e_x^{\text{LR-DFA}}(\vec{r}, \omega(\vec{r}))] \quad (44)$$

If  $\omega(\vec{r})$  is chosen to be a constant, this reduces to a conventional range-separated hybrid. Though there is no real reason to think it would be formally superior to the previous approach, we note that range-separated hybrids have been more thoroughly investigated than have local hybrids -- in other words, we have somewhat greater insight into what we should pick for  $\omega(\vec{r})$  than we do for choosing  $c(\vec{r})$ .

The chief difficulty lies in evaluating  $e_x^{\text{SR-HF}}(\vec{r}, \omega(\vec{r}))$  and  $e_x^{\text{LR-HF}}(\vec{r}, \omega(\vec{r}))$ . These quantities require, in principle,  $O(N_{\text{AO}}^2)$  integrations at each point  $\vec{r}$ , where  $N_{\text{AO}}$  is the size of the atomic orbital basis set used to expand the Kohn–Sham molecular orbitals. The cost of evaluating the total exchange energy is thus  $O(N_{\text{grid}} N_{\text{AO}}^2)$ , where  $N_{\text{grid}}$  is the size of the numerical integration grid used to integrate with respect to  $\vec{r}$ . This cost is unacceptably high for most applications.

In conventional local hybrids, one can reduce the computational scaling considerably by writing

$$e_x^{\text{HF}}(\vec{r}, \omega) = -\frac{1}{2} \sum_{ij} \varphi_i(\vec{r}) \int d\vec{r}' d\vec{r}'' \varphi_j(\vec{r}'') \times \frac{\varphi_i(\vec{r}') \varphi_j(\vec{r}')}{|\vec{r}'' - \vec{r}'|} \delta(\vec{r} - \vec{r}'') \quad (45)$$

and replacing the  $\delta$  function with a completeness insertion, as proposed by Della Sala and Görling.<sup>124</sup> If the states in the completeness insertion are chosen to be the atomic orbitals, this yields

$$e_x^{\text{HF}}(\vec{r}) = \frac{1}{2} \sum_{\mu, \nu} \chi_{\mu}(\vec{r}) Q_{\mu\nu} \chi_{\nu}(\vec{r}) \quad (46)$$

Here,  $\chi_{\mu}(\vec{r})$  and  $\chi_{\nu}(\vec{r})$  are basis functions and  $2\mathbf{Q} = \mathbf{S}^{-1} \mathbf{K} \mathbf{P} + \mathbf{PKS}^{-1}$ , where  $\mathbf{S}$  is the basis function overlap matrix,  $\mathbf{K}$  is the conventional Hartree–Fock exchange operator matrix, and  $\mathbf{P}$  is the density matrix for the system of interest. This trick makes evaluating  $e_x^{\text{HF}}(\vec{r})$  no more expensive than evaluating  $\rho(\vec{r})$ , except for the minor additional overhead of computing  $\mathbf{Q}$  once per SCF iteration. We point out that, as the Della Sala–Görling form of the exact exchange energy density correctly integrates to the total exchange energy, it merely corresponds to a particular choice of gauge.

This completeness insertion can also be used for range-separated local hybrids with constant  $\omega$  by simply replacing the standard two-electron integrals in the matrix  $\mathbf{K}$  by the

corresponding range-separated integrals. However, if  $\omega$  is a function of space, this is no longer practical. It requires a different matrix  $\mathbf{Q}$  at every point in space, and the completeness insertion saves us no time at all.

To resolve this problem, Krukau, Scuseria, Savin, and Perdew proposed that a semilocal exchange hole model be used in place of the exact exchange hole, but that it be parametrized to reproduce the full-range exact exchange energy.<sup>98</sup> This model is then used to build an approximate range-separated exact exchange energy density, and is exact for  $\omega = 0$  and  $\omega = \infty$ . Preliminary results are encouraging - a range-separated hybrid of short-range LSDA and long-range exact exchange with a position-dependent  $\omega$  gives results roughly comparable to LC- $\omega$ PBE for small thermochemical test sets. More investigation is necessary before any general conclusions can be drawn.

**4.4. Other Advances.** In this final section, we discuss a few hybrid functionals developed by other groups that provide interesting perspectives on our own work. One such area is the explicit nonlocal treatment of nondynamical correlation. As discussed in section 3.3, semilocal density functionals for exchange can mimic nondynamical correlation in covalent bonds. However, these functionals are also plagued by self-interaction error, and their incorporation of nondynamical correlation effects is quite approximate. As functionals continue to advance, it becomes desirable to eliminate SIE and use full nonlocal exact exchange. This, however, requires us to explicitly account for nondynamical correlation. Nonlocal functionals which do so, and thus complement nonlocal exact exchange, now exist.<sup>132–135</sup>

A second area of progress is in hybrid functionals constructed from more sophisticated treatments of the adiabatic connection<sup>136,137</sup> between the real system of interest and the noninteracting Kohn–Sham system. The adiabatic connection allows us to write

$$E_{xc}[\rho] = \int_0^1 d\lambda W_\lambda[\rho] \quad (47)$$

where

$$W_\lambda[\rho] = \langle \Psi_{\rho,\lambda} | V_{ee} | \Psi_{\rho,\lambda} \rangle - U[\rho] \quad (48)$$

and where  $|\Psi_{\rho,\lambda}\rangle$  is that wave function which yields density  $\rho$  and minimizes  $\langle \hat{T} + \lambda \hat{V}_{ee} \rangle$ . The wave function at  $\lambda = 0$  is the Kohn–Sham determinant, and  $W_0[\rho]$  is thus the exact exchange energy functional. If we approximate  $W_1[\rho]$  with a semilocal exchange-correlation functional, then a global hybrid can be derived from the coupling-constant integral of eq 46 by approximating  $W_\lambda[\rho]$  in terms of  $W_0[\rho]$  and  $W_1[\rho]$ .

One such approximation<sup>137</sup> is

$$W_\lambda[\rho] \approx W_0[\rho] + \lambda^p (W_1[\rho] - W_0[\rho]) \quad (49)$$

Under this assumption, we have

$$E_{xc}[\rho] = W_0[\rho] + \frac{1}{1+p} (W_1[\rho] - W_0[\rho]) \quad (50)$$

Simplifying, and using  $W_0[\rho] = E_x^{\text{HF}}$  and  $W_1[\rho] = E_{xc}^{\text{DFA}}$ , we obtain the conventional global hybrid formulation of Eqn. 10, with  $c = p/(1+p)$ .

Notice, however, that nothing forces us to make such a simple ansatz for the dependence on  $\lambda$ . By considering more complicated forms for  $W_\lambda[\rho]$ , as proposed by Ernzerhof<sup>138</sup> and collaborators,<sup>139</sup> more general hybrid functionals can be developed, including those which eliminate one-electron SIE. This is the route taken by the MCY family of functionals of Morisánchez, Cohen, and Yang.<sup>130,140,141</sup>

The ultimate possible accuracy of hybrids, whether hybrids of exact exchange and GGAs or of exact exchange and meta-GGAs, is an important question. To answer it, Zhao and Truhlar have developed the M06 family of functionals, which combine carefully chosen functional forms and extensive empirical parametrization to achieve broad-ranging accuracy for thermochemistry, reaction barriers, noncovalent interactions, electronic spectroscopy, and transition metal binding.<sup>5,49,60</sup>

## 5. Conclusions and Future Perspectives

Kohn–Sham DFT has made remarkable progress from its initial local density realization to the present day. That progress is due largely to advances in exchange-correlation functionals, and particularly to the advent of hybrid functionals. We have long since reached the point that KS-DFT is sufficiently accurate to supplant ab initio wave function techniques as the method of choice for most purposes. Challenges remain, and universally affordable and accurate functionals still elude us.

However, significant progress in the development of more robust, general-purpose functionals has been made in the past decade. We continue to advance up the Jacob’s ladder of exchange-correlation functionals. Functionals now exist to describe nondynamical correlation. We have begun to understand how to limit self-interaction error, both one-electron and many-electron. Continuing that progress in functional development is of crucial importance.

Range-separated hybrids are an important and growing area of investigation, while local hybrids are beginning to come into their own. These and other carefully tailored hybrid functionals show significant promise for ongoing development. By including the right amount of nonlocal exchange in the right places, functionals can be constructed with the right physics, and this, ultimately, is what we need.

**Acknowledgment.** This work was supported by the National Science Foundation (CHE-0807194), the Department of Energy (DE-FG02-04ER15523), the Army Research Office (MURI DAAD-19-03-1-0169), and the Welch Foundation (C-0036). B.G.J. acknowledges additional support from a training fellowship from the National Library of Medicine to the Keck Center for Interdisciplinary Bioscience Training of the Gulf Coast Consortium (NLM Grant No. 5T15LM07093).

## Appendix: The Exchange-Correlation Hole

The exchange-correlation hole is an important concept in DFT. It helps explain the physics of nondynamical correlation, and it can be used as a guide to constructing functionals. We do not wish to discuss it here in any great detail, but a brief review may be in order.

We begin by considering the pair density  $\rho_2(\vec{r}_1, \vec{r}_2)$ , which, omitting normalization, yields the probability of simultaneously finding one electron at  $\vec{r}_1$  and another at  $\vec{r}_2$ . In terms of the wave function  $\Psi(\vec{r}_1, \vec{r}_2, \dots)$  it is given as

$$\rho_2(\vec{r}_1, \vec{r}_2) = \frac{N(N-1)}{2} \int d\vec{r}_3 \dots d\vec{r}_N \Psi(\vec{r}_1, \vec{r}_2, \vec{r}_3, \dots, \vec{r}_N) \times \Psi(\vec{r}_1, \vec{r}_2, \vec{r}_3, \dots, \vec{r}_N) \quad (\text{A-1})$$

It can be decomposed into a part which is exact for statistically independent identical particles and a part which accounts for the correlations, via

$$\rho_2(\vec{r}_1, \vec{r}_2) = \frac{1}{2} \rho(\vec{r}_1) \rho(\vec{r}_2) (1 + g_{xc}(\vec{r}_1, \vec{r}_2)) \quad (\text{A-2})$$

This defines the pair correlation function  $g_{xc}(\vec{r}_1, \vec{r}_2)$ . The electron–electron interaction energy can be evaluated simply as

$$E_{ee} = \int d\vec{r}_1 d\vec{r}_2 \frac{\rho_2(\vec{r}_1, \vec{r}_2)}{r_{12}}$$

$$= \frac{1}{2} \int dr_1 d\vec{r}_2 \rho(\vec{r}_1) \rho(\vec{r}_2) \frac{1 + g_{xc}(\vec{r}_1, \vec{r}_2)}{r_{12}} \quad (\text{A-3})$$

That part independent of the pair-correlation function yields the usual Coulomb interaction term  $U[\rho]$ .

To define the exchange-correlation hole, we write

$$h_{xc}(\vec{r}_1; \vec{r}_{12}) = \rho(\vec{r}_2) g_{xc}(\vec{r}_1, \vec{r}_2) \quad (\text{A-4})$$

Physically, it represents a charge distribution with which a test electron located at  $\vec{r}_1$  interacts Coulombically; a “hole” in the  $N$ -electron density  $\rho(\vec{r}_2)$  which adds self-interaction and exchange-correlation effects to the classical Coulomb interaction between the test electron and  $\rho(\vec{r}_2)$ . Since the Coulomb term  $U[\rho]$  allows each electron to interact with all  $N$  electrons when physically each electron interacts only with the  $N - 1$  other electrons, the exchange-correlation represents a one-electron hole in  $\rho(\vec{r}_2)$ .

We can separate the exact exchange hole from the correlation hole by using the one-particle density matrix  $\rho_1(\vec{r}_1; \vec{r}_2)$  defined in terms of the occupied molecular orbitals  $\{\phi_i(\vec{r})\}$  of eq 5 as

$$\rho_1(\vec{r}_1; \vec{r}_2) = \sum_i^{\text{occ}} \varphi_i(\vec{r}_1) \varphi_i(\vec{r}_2) \quad (\text{A-5})$$

The exact exchange hole is then defined by

$$\rho(\vec{r}_1) h_x(\vec{r}_1; \vec{r}_{12}) = -\rho_1(\vec{r}_1; \vec{r}_2) \rho_1(\vec{r}_2; \vec{r}_1) \quad (\text{A-6})$$

and integrates to the exact exchange energy.

There are many known constraints on the exchange and correlation holes, but most important are the following integrations:

- The exchange-correlation energy can be extracted from the exchange-correlation hole by

$$E_{xc} = \frac{1}{2} \int d\vec{r}_1 d\vec{r}_2 \frac{\rho(\vec{r}_1) h_{xc}(\vec{r}_1; \vec{r}_{12})}{r_{12}} \quad (\text{A-7})$$

with analogous expressions holding individually for the exchange and correlation components.

- The exchange-correlation hole is normalized at each point in space, so that

$$\int d\vec{r}_2 h_{xc}(\vec{r}_2; \vec{r}_{12}) = -1 \quad (\text{A-8})$$

Except in fractionally charged systems, there are separate normalization conditions on the exchange and correlation holes, namely

$$\int d\vec{r}_1 h_x(\vec{r}_1; \vec{r}_{12}) = -1 \quad (\text{A-9a})$$

$$\int d\vec{r}_2 h_c(\vec{r}_1; \vec{r}_{12}) = 0 \quad (\text{A-9b})$$

Physically, this tells us that the correlation hole about  $\vec{r}_1$  represents a reorganization of the density  $\rho(\vec{r}_2)$  to account for correlation effects, while the exchange hole about  $\vec{r}_1$  not only adds reorganization effects due to exchange but also removes the artificial self-interaction in the Coulomb term.

## References and Notes

- (1) Parr, R. G.; Yang, W. *Density Functional Theory of Atoms and Molecules*; Oxford University Press: New York, 1989.
- (2) Dreizler, R. M.; Gross, E. K. U. *Density Functional Theory*; Plenum Press: New York, 1995.
- (3) Scuseria, G. E.; Staroverov, V. N. Progress in the development of exchange-correlation functionals In *Theory and Applications of Com-*

*putational Chemistry: The First 40 Years*; Dykstra, C. E., Frenking, G., Kim, K. S., Scuseria, G. E., Eds.; Elsevier: Amsterdam, The Netherlands, 2005.

- (4) Dreuw, A.; Head-Gordon, M. *Chem. Rev.* **2006**, *105*, 4009.
- (5) Zhao, Y.; Truhlar, D. G. *J. Phys. Chem. A* **2006**, *110*, 13126.
- (6) Peach, M. J. G.; Benfield, P.; Helgaker, T.; Tozer, D. J. *J. Chem. Phys.* **2008**, *128*, 044118.
- (7) Perdew, J. P.; Ruzsinszky, A.; Tao, J.; Staroverov, V. N.; Scuseria, G. E.; Csonka, G. I. *J. Chem. Phys.* **2005**, *123*, 062201.
- (8) Perdew, J. P.; Schmidt, K. In *Density Functional Theory and Its Applications to Materials*; American Institute of Physics: New York, 2001.
- (9) Hohenberg, P.; Kohn, W. *Phys. Rev.* **1964**, *136*, B864.
- (10) Ivanov, S.; Hirata, S.; Bartlett, R. J. *Phys. Rev. Lett.* **1999**, *83*, 5455.
- (11) Görling, A. *Phys. Rev. Lett.* **1999**, *83*, 5459.
- (12) Yang, W.; Wu, Q. *Phys. Rev. Lett.* **2002**, *89*, 143002.
- (13) Grabowski, I.; Hirata, S.; Ivanov, S.; Bartlett, R. J. *J. Chem. Phys.* **2002**, *116*, 4415.
- (14) Bartlett, R. J.; Grabowski, I.; Hirata, S.; Ivanov, S. *J. Chem. Phys.* **2005**, *122*, 034104.
- (15) Bartlett, R. J.; Schweigert, I. V.; Lotrich, V. F. *J. Mol. Struct.: THEOCHEM* **2006**, *771*, 1.
- (16) Pople, J. A.; Head-Gordon, M.; Fox, D. J.; Raghavachari, K.; Curtiss, L. A. *J. Chem. Phys.* **1989**, *90*, 5622.
- (17) Curtiss, L. A.; Jones, C.; Trucks, G. W.; Raghavachari, K.; Pople, J. A. *J. Chem. Phys.* **1990**, *93*, 2537.
- (18) Curtiss, L. A.; Raghavachari, K.; Redfern, P. C.; Pople, J. A. *J. Chem. Phys.* **1997**, *106*, 1063.
- (19) Curtiss, L. A.; Redfern, P. C.; Raghavachari, K.; Pople, J. A. *J. Chem. Phys.* **1998**, *109*, 42.
- (20) Curtiss, L. A.; Raghavachari, K.; Redfern, P. C.; Pople, J. A. *J. Chem. Phys.* **2000**, *112*, 7374.
- (21) Curtiss, L. A.; Redfern, P. C.; Raghavachari, K.; Pople, J. A. *J. Chem. Phys.* **2001**, *114*, 108.
- (22) Zhao, Y.; Lynch, B. J.; Truhlar, D. G. *Phys. Chem. Chem. Phys.* **2004**, *7*, 43.
- (23) Zhao, Y.; González-García, N.; Truhlar, D. G. *J. Phys. Chem. A* **2005**, *109*, 2012. Zhao, Y.; González-García, N.; Truhlar, D. G. *J. Phys. Chem. A* **2006**, *110*, 4942; Erratum.
- (24) Chakravorty, S. J.; Gwaltney, S. R.; Davidson, E. R.; Parpia, F. A.; Fischer, C. F. *Phys. Rev. A* **1993**, *47*, 3649.
- (25) Lynch, B. J.; Truhlar, D. G. *J. Phys. Chem. A* **2003**, *107*, 8996.
- (26) Ceperly, D. M.; Alder, B. J. *Phys. Rev. Lett.* **1980**, *45*, 566.
- (27) Sovko, S. H.; Wilk, I.; Nusair, M. *Canadian J. Phys.* **1980**, *58*, 1200.
- (28) Perdew, J. P.; Wang, Y. *Phys. Rev. B* **1992**, *45*, 13244.
- (29) Gell-Mann, M.; Brueckner, K. A. *Phys. Rev.* **1957**, *106*, 364.
- (30) Khein, A.; Singh, D. J.; Umrigar, C. *Phys. Rev. B* **1995**, *51*, 4105.
- (31) Kurth, S.; Perdew, J. P.; Blaha, P. *Int. J. Quantum Chem.* **1999**, *75*, 889.
- (32) Perdew, J. P. *Int. J. Quantum Chem. Symp* **1986**, *19*, 497.
- (33) Casida, M. E.; Jamorski, C.; Casida, K. C.; Salahub, D. R. *J. Chem. Phys.* **1998**, *108*, 4439.
- (34) Ma, S.-K.; Brueckner, K. A. *Phys. Rev.* **1968**, *165*, 18.
- (35) Perdew, J. P.; Wang, Y. *Phys. Rev. B* **1986**, *33*, 8800. Perdew, J. P.; Wang, Y. *Phys. Rev. B* **1986**, *40*, 3399; Erratum.
- (36) Perdew, J. P. *Phys. Rev. B* **1986**, *33*, 8822. Perdew, J. P. *Phys. Rev. B* **1986**, *34*, 7406; Erratum.
- (37) Langreth, D. C.; Mehl, M. J. *Phys. Rev. Lett.* **1981**, *47*, 446.
- (38) Becke, A. D. *Phys. Rev. A* **1988**, *38*, 3098.
- (39) Lee, C.; Yang, W.; Parr, R. G. *Phys. Rev. B* **1998**, *37*, 785.
- (40) Perdew, J. P.; Burke, K.; Ernzerhof, M. *Phys. Rev. Lett.* **1996**, *77*, 3865. Perdew, J. P.; Burke, K.; Ernzerhof, M. *Phys. Rev. Lett.* **1997**, *78*, 1396; Erratum.
- (41) Perdew, J. P. In *Electronic Structure of Solids*; Ziesche, P., Eschrig, H., Eds.; Akademie Verlag: Berlin, 1991.
- (42) Miehlisch, B.; Savin, A.; Stoll, H.; Preuss, H. *Chem. Phys. Lett.* **1989**, *157*, 200.
- (43) Proynov, E. I.; Ruiz, E.; Vela, A.; Salahub, D. R. *Int. J. Quantum Chem. Symp.* **1995**, *29*, 61.
- (44) Ozolins, V.; Körling, M. *Phys. Rev. B* **1993**, *48*, 18304.
- (45) Filippi, C.; Singh, D. J.; Umrigar, C. *Phys. Rev. B* **1994**, *50*, 14947.
- (46) Voorhis, T. V.; Scuseria, G. E. *J. Chem. Phys.* **1998**, *109*, 400.
- (47) Perdew, J. P.; Kurth, S.; Zupan, A.; Blaha, P. *Phys. Rev. Lett.* **1998**, *82*, 2544.
- (48) Tao, J.; Perdew, J. P.; Staroverov, V. N.; Scuseria, G. E. *Phys. Rev. Lett.* **2003**, *91*, 146401.
- (49) Zhao, Y.; Truhlar, D. G. *J. Chem. Phys.* **2006**, *125*, 194101.
- (50) Becke, A. D. *J. Chem. Phys.* **1993**, *98*, 1372.
- (51) Becke, A. D. *J. Chem. Phys.* **1993**, *98*, 5648.
- (52) Sharp, R. T.; Horton, G. K. *Phys. Rev.* **1953**, *90*, 317.
- (53) Talman, J. D.; Shadwick, W. F. *Phys. Rev. A* **1976**, *14*, 36.

- (54) Seidl, A.; Görling, A.; Vogl, P.; Majewski, J. A.; Levy, M. *Phys. Rev. B* **1996**, *53*, 3764.
- (55) Neumann, R.; Nobes, R. H.; Handy, N. C. *Mol. Phys.* **1996**, *87*, 1.
- (56) Stephens, P. J.; Devlin, F. J.; Chabalowski, C. F.; Frisch, M. J. *J. Phys. Chem.* **1994**, *98*, 11623.
- (57) Ernzerhof, M.; Scuseria, G. E. *J. Chem. Phys.* **1999**, *110*, 5029.
- (58) Staroverov, V. N.; Scuseria, G. E.; Tao, J.; Perdew, J. P. *J. Chem. Phys.* **2003**, *119*, 12129.
- (59) Lynch, B. J.; Fast, P. L.; Harris, M.; Truhlar, D. G. *J. Phys. Chem. A* **2000**, *104*, 4811.
- (60) Zhao, Y.; Truhlar, D. G. *Theor. Chem. Acc.* **2008**, *120*, 215.
- (61) Champagne, B.; Perpete, E. A.; van Gisbergen, S. J. A.; Baerends, E.-J.; Snijders, J. G.; Soubra-Ghaoui, C.; Robins, K. A.; Kirtman, B. *J. Chem. Phys.* **1998**, *109*, 10489.
- (62) Monkhorst, H. J. *Phys. Rev. B* **1979**, *20*, 1504.
- (63) Heyd, J.; Scuseria, G. E.; Ernzerhof, M. *J. Chem. Phys.* **2003**, *118*, 8207.
- (64) Paier, J.; Marsman, M.; Kresse, G.; Gerber, I. C.; Ángyán, J. G. *J. Chem. Phys.* **2006**, *124*, 154709.
- (65) Perdew, J. P.; Zunger, A. *Phys. Rev. B* **1981**, *23*, 5048.
- (66) Ruzsinszky, A.; Perdew, J. P.; Csonka, G. I.; Vydrov, O. A.; Scuseria, G. E. *J. Chem. Phys.* **2006**, *125*, 194112.
- (67) Mori-Sánchez, P.; Cohen, A. J. *J. Chem. Phys.* **2006**, *125*, 201102.
- (68) Vydrov, O. A.; Scuseria, G. E.; Perdew, J. P. *J. Chem. Phys.* **2007**, *126*, 154109.
- (69) Cohen, A. J.; Mori-Sánchez, P.; Yang, W. *Phys. Rev. B* **2008**, *77*, 115123.
- (70) Mori-Sánchez, P.; Cohen, A. J.; Yang, W. *Phys. Rev. Lett.* **2008**, *100*, 146401.
- (71) Johnson, B. G.; Gonzalez, C. A.; Gill, P. M. W.; Pople, J. A. *Chem. Phys. Lett.* **1994**, *221*, 100.
- (72) Csonka, G. I.; Johnson, B. G. *Theor. Chem. Acc.* **1998**, *99*, 158.
- (73) Patchkovskii, S.; Ziegler, T. *J. Chem. Phys.* **2002**, *116*, 7806.
- (74) Janesko, B. G.; Scuseria, G. E. *J. Chem. Phys.* **2008**, *128*, 24112.
- (75) Iikura, H.; Tsuneda, T.; Yanai, T.; Hirao, K. *J. Chem. Phys.* **2001**, *115*, 3540.
- (76) Tawada, Y.; Tsuneda, T.; Yanagisawa, S.; Yanai, T.; Hirao, K. *J. Chem. Phys.* **2004**, *120*, 8425.
- (77) Sekino, H.; Maeda, Y.; Kamiya, M. *Mol. Phys.* **2005**, *103*, 2183.
- (78) Vydrov, O. A.; Scuseria, G. E. *J. Chem. Phys.* **2006**, *125*, 234109.
- (79) Perdew, J. P.; Parr, R. G.; Levy, M.; J. L.; Balduz, J. *Phys. Rev. Lett.* **1982**, *49*, 1691.
- (80) Slater, J. C. *Phys. Rev.* **1951**, *81*, 385.
- (81) Baerends, E. J. *Phys. Rev. Lett.* **2001**, *87*, 133004.
- (82) Savin, A.; Flad, H.-J. *Int. J. Quantum Chem.* **1995**, *56*, 327.
- (83) Savin, A. On degeneracy, near-degeneracy and density functional theory In *Recent Developments and Applications of Modern Density Functional Theory*; Seminario, J. M., Ed.; Elsevier: Amsterdam, The Netherlands, 1996.
- (84) Leininger, T.; Stoll, H.; Werner, H.-J.; Savin, A. *Chem. Phys. Lett.* **1997**, *275*, 151.
- (85) Song, J.-W.; Hirose, T.; Tsuneda, T.; Hirao, K. *J. Chem. Phys.* **2007**, *126*, 154105.
- (86) Heyd, J.; Scuseria, G. E.; Ernzerhof, M. *J. Chem. Phys.* **2006**, *124*, 219906.
- (87) Gerber, I. C.; Ángyán, J. G. *Chem. Phys. Lett.* **2005**, *415*, 100.
- (88) Gerber, I. C.; Ángyán, J. G.; Marsman, M.; Kresse, G. *J. Chem. Phys.* **2007**, *127*, 054101.
- (89) Burke, K.; Cruz, F. G.; Lam, K.-C. *J. Chem. Phys.* **1998**, *109*, 8161.
- (90) Jaramillo, J.; Scuseria, G. E.; Ernzerhof, M. *J. Chem. Phys.* **2003**, *118*, 1068.
- (91) Janesko, B. G.; Scuseria, G. E. *J. Chem. Phys.* **2007**, *127*, 164117.
- (92) Kaupp, M.; Bahmann, H.; Arbuznikov, A. V. *J. Chem. Phys.* **2007**, *127*, 194102.
- (93) Janesko, B. G.; Scuseria, G. E. *J. Chem. Phys.* **2008**, *128*, 084111.
- (94) Ernzerhof, M.; Perdew, J. P. *J. Chem. Phys.* **1998**, *109*, 3313.
- (95) Henderson, T. M.; Janesko, B. G.; Scuseria, G. E. *J. Chem. Phys.* **2008**, *128*, 194105.
- (96) Bahmann, H.; Ernzerhof, M. *J. Chem. Phys.* **2008**, *128*, 234104.
- (97) Constantin, L. A.; Perdew, J. P.; Tao, J. *Phys. Rev. B* **2006**, *73*, 205104.
- (98) Krukau, A. V.; Scuseria, G. E.; Perdew, J. P.; Savin, A. *J. Chem. Phys.* **2008**, *129*, 124103.
- (99) Gill, P. M. W.; Adamson, R. D.; Pople, J. A. *Mol. Phys.* **1996**, *88*, 1005.
- (100) Toulouse, J.; Colonna, F.; Savin, A. *Phys. Rev. A* **2004**, *70*, 062505.
- (101) Toulouse, J.; Savin, A.; Flad, H.-J. *Int. J. Quantum Chem.* **2004**, *100*, 1047.
- (102) Henderson, T. M.; Bartlett, R. J. *Phys. Rev. A* **2004**, *70*, 022512.
- (103) Toulouse, J.; Colonna, F.; Savin, A. *J. Chem. Phys.* **2005**, *122*, 014110.
- (104) Goll, E.; Werner, H.-J.; Stoll, H. *Phys. Chem. Chem. Phys.* **2005**, *7*, 3917.
- (105) Adamo, C.; Barone, V. *J. Chem. Phys.* **1999**, *110*, 6158.
- (106) Delhalle, J.; Calais, J.-L. *Phys. Rev. B* **1987**, *35*, 9460.
- (107) Zecca, L.; Gori-Giorgi, P.; Moroni, S.; Bachelet, G. B. *Phys. Rev. B* **2004**, *70*, 205127.
- (108) Heyd, J.; Scuseria, G. E. *J. Chem. Phys.* **2004**, *120*, 7274.
- (109) Heyd, J.; Scuseria, G. E. *J. Chem. Phys.* **2004**, *121*, 1187.
- (110) Heyd, J.; Peralta, J. E.; Scuseria, G. E.; Martin, R. L. *J. Chem. Phys.* **2005**, *123*, 174101.
- (111) Bredow, T.; Gerson, A. R. *Phys. Rev. B* **2000**, *61*, 5194.
- (112) Muscat, J.; Wander, A.; Harrison, N. M. *Chem. Phys. Lett.* **2001**, *342*, 397.
- (113) Batista, E.; Heyd, J.; Hennig, R. G.; Uberuaga, B. P.; Martin, R. L.; Scuseria, G. E.; Umrigar, C. J. *Phys. Rev. B* **2006**, *74*, 121102.
- (114) Hay, P. J.; Martin, R. L.; Uddin, J.; Scuseria, G. E. *J. Chem. Phys.* **2006**, *125*, 034712.
- (115) Prodan, I. D.; Scuseria, G. E.; Martin, R. L. *Phys. Rev. B* **2006**, *73*, 045104.
- (116) da Silva, J. R. F.; Gangaduglia-Pirovana, M. V.; Sauer, J.; Bayer, V.; Kresse, G. *Phys. Rev. B* **2007**, *75*, 045121.
- (117) Prodan, I. D.; Scuseria, G. E.; Martin, R. L. *Phys. Rev. B* **2007**, *76*, 033103.
- (118) Paier, J.; Marsman, M.; Kresse, G. *J. Chem. Phys.* **2007**, *127*, 024103.
- (119) Henderson, T. M.; Izmaylov, A. F.; Scuseria, G. E.; Savin, A. *J. Chem. Phys.* **2007**, *127*, 221103.
- (120) Henderson, T. M.; Izmaylov, A. F.; Scuseria, G. E.; Savin, A. *J. Chem. Theory Comput.* **2008**, *4*, 1254.
- (121) Tao, J.; Staroverov, V. N.; Scuseria, G. E.; Perdew, J. P. *Phys. Rev. A* **2008**, *77*, 012509.
- (122) Bahmann, H.; Rodenberg, A.; Arbuznikov, A. V.; Kaupp, M. *J. Chem. Phys.* **2007**, *126*, 011103.
- (123) Arbuznikov, A. V.; Kaupp, M. *Chem. Phys. Lett.* **2007**, *440*, 160.
- (124) Della Sala, F.; Görling, A. *J. Chem. Phys.* **2001**, *115*, 5718.
- (125) Gritsenko, O. V.; Baerends, E. J. *Phys. Rev. A* **2001**, *64*, 042506.
- (126) Krieger, J. B.; Li, Y.; Iafate, G. J. *Phys. Rev. A* **1992**, *45*, 101.
- (127) Arbuznikov, A. V.; Kaupp, M.; Bahmann, H. *J. Chem. Phys.* **2006**, *124*, 204102.
- (128) Arbuznikov, A. V.; Kaupp, M. *Chem. Phys. Lett.* **2007**, *442*, 496.
- (129) Arbuznikov, A. V.; Kaupp, M. *J. Chem. Phys.* **2008**, *128*, 214107.
- (130) Cohen, A.; Mori-Sánchez, P.; Yang, W. *J. Chem. Phys.* **2007**, *126*, 191109.
- (131) Janesko, B. G.; Krukau, A. V.; Scuseria, G. E. *J. Chem. Phys.* **2008**, *129*, 124110.
- (132) Dion, M.; Rydberg, H.; Schröder, E.; Langreth, D. C.; Lundqvist, B. I. *Phys. Rev. Lett.* **2004**, *92*, 246401. Dion, M.; Rydberg, H.; Schröder, E.; Langreth, D. C.; Lundqvist, B. I. *Phys. Rev. Lett.* **2005**, *95*, 109902; Erratum.
- (133) Becke, A. D. *J. Chem. Phys.* **2005**, *122*, 064101.
- (134) Becke, A. D.; Johnson, E. R. *J. Chem. Phys.* **2007**, *127*, 124108.
- (135) Johnson, E. R.; Becke, A. D. *J. Chem. Phys.* **2008**, *128*, 124105.
- (136) Langreth, D. C.; Perdew, J. P. *Phys. Rev. B* **1977**, *15*, 2884.
- (137) Perdew, J. P.; Ernzerhof, M.; Burke, K. *J. Chem. Phys.* **1996**, *105*, 9982.
- (138) Ernzerhof, M. *Chem. Phys. Lett.* **1996**, *263*, 499.
- (139) Burke, K.; Ernzerhof, M.; Perdew, J. P. *Chem. Phys. Lett.* **1997**, *265*, 115.
- (140) Mori-Sánchez, P.; Cohen, A. J.; Yang, W. *J. Chem. Phys.* **2006**, *124*, 091102.
- (141) Cohen, A. J.; Mori-Sánchez, P.; Yang, W. *J. Chem. Phys.* **2007**, *127*, 034101.